# Model test of Pile-plank structure working as Roadbed of High Speed Railway overlying Goafs

Qian-gong CHENG(1,*), Yan LI(1), Jian-lei ZHANG(1), Yu-feng WANG(1), and Xin LIANG(1,2)

(1) Department of Geological Engineering, Southwest Jiaotong University, Chengdu, China;
Correspondence to Qian-gong CHENG,
E-mail: chengqiangong@swjtu.edu.cn
(2) Faculty of Civil Engineering, Guangxi University of Science and Technology, Liuzhou, China

**Abstract**

Based on abundant data obtained by the physical model tests of pile-plank structure used as composite foundation of Wufushan station which overlies goafs in Hefei-Fuzhou high speed railway, the distributions of pile axial force, earth pressure and settlements were obtained. The results suggest: (1) the axial force at pile head was maximum, while the value at the depth where the goafs locate remained constant as the pile was subjected to loads. And the value of axial force decreased as the depth of pile increased. (2) With the increase of depth of pile, the value of skin friction of pile also decreased, and there was no skin friction along the sections where the pile crosses the goafs. Besides, no negative skin friction appeared. (3) The change of pile-soil stress ratio was consistent with the pile-soil load share ratio. The load shared by piles grew gradually as loads increased, and eventually reached a stable value. (4) The bearing plank and soils between piles settled uniformly, with a small value. The settlements of roadbeds overlying goafs and non-goafs were almost same, and there was no deformation at the bottom of goaf roofs. (5) The pile-plank structure had a good effect on the roadbed remedy.

**Keywords:** high-speed railway; goaf; pile-plank roadbed; model test; stress; settlement

## 1. Introduction

It is compulsory for a high speed railway to control settlement of its roadbed. If there are great areas of goafs, the railway will bypass those goafs, otherwise, grouting will be implemented. Sometimes, the foundation overlying the goafs will be reinforced. Hefei-Fuzhou high speed railway, design speed of 350km, overlies goafs which locate in Shangrao of Jiangxi Province. In order to control the deformation of the superstructure, a pile-plank structure was used to reinforce the foundation. As a new remedial measure of weak foundations, the pile-plank structure has been applied to many high speed railways in China, such as the Beijing-Tianjin intercity railway (Shen, et al., 2009; Jing, 2006), the Beijing-Shanghai high speed railway (Zhang, et al., 2011; Xu, et al., 2012), the Wuhan-Guangzhou high speed railway (Zhan, et al., 2007), the Zhengzhou-Xi'an high speed railway (Su, et al., 2012), and the Suining-Chongqing high speed railway (Zhan, et al., 2008). The effectiveness of the pile-plank structure in such high speed railways is pretty well, however, there are few cases where pile-plank structures are used as a reinforced foundation when the railway overlies goafs, so it is necessary to understand this remedial measure. Wufushan station in the Hefei-Fuzhou high speed railway locates in the Sishiba town of Shangrao of Jiangxi Province. The goafs underlying the roadbed were produced by coal mining before 1949 and during 1980s. This paper studies the settlement characteristic of the foundation, the mechanism of the load transmission and the interaction between pile and plank by a physical model test.

## 2. Project profile

The prototype cross section of the model test locates at DK499+940 of the Hefei-Fuzhou high speed railway, and the strata under the station are as follows: layer① is completely weathering sandstone; layer② is intensely weathering sandstone; and layer ③ is moderately weathering limestone. And there are two goafs: No.1 goaf, 2.0 m in height and 2.5 m in width, locates on the left of the cross section at the depth of 10.5~12.5 m, and the No.2 goaf, 2.8 m in height and 2.5 m in width, locates in the middle of the cross section at the depth of 19.8~22.6 m. Besides, 3.0-meter-high embankment fill materials, which are composed of 3% cement and grade crushed gravels, lies on the top of a 1.2-meter-thick bearing plank, and the slope rate is 1:1.5. The locations of strata, goafs and piles are shown in Fig.1(a), where A~D are the numbers of rails, while I ~ VII are the numbers of piles

Table 1 Pile length and traversing strata at prototype section

| Pile number | Pile length/m | Depth /m | Strata | Bearing layer | Goafs depth /m |
|---|---|---|---|---|---|
| I | 12 | 0.00~5.87 | completely weathering sandstone | moderately weathering limestone | 10.5~12.5 |
| | | 5.87~8.76 | intensely weathering sandstone | | |
| | | 8.76~12.00 | moderately weathering limestone | | |
| □ | 20 | 0.00~2.46 | completely weathering sandstone | intensely weathering sandstone | |
| | | 2.46~20.00 | intensely weathering sandstone | | |
| □ | 25 | 0.00~2.31 | completely weathering sandstone | intensely weathering sandstone | |
| | | 2.31~25.00 | intensely weathering sandstone | | |
| □ | 24 | 0.00~4.23 | completely weathering sandstone | moderately weathering limestone | 19.8~22.6 |
| | | 4.23~19.58 | intensely weathering sandstone | | |
| | | 19.58~24.00 | moderately weathering limestone | | |
| □~ VII | 25 | 0.00~2.58 | completely weathering sandstone | intensely weathering sandstone | |
| | | 2.58~25.00 | intensely weathering sandstone | | |

which are 12, 20, 25, 24, 25, 25, 25 m in length respectively. The pile diameter is 1.0 m, and the distance of pile-to-pile is 5.0 m. The configuration of the pile-plank structure is shown in Fig.1(b). The information of piles and the strata piles pass through is shown in Table 1.

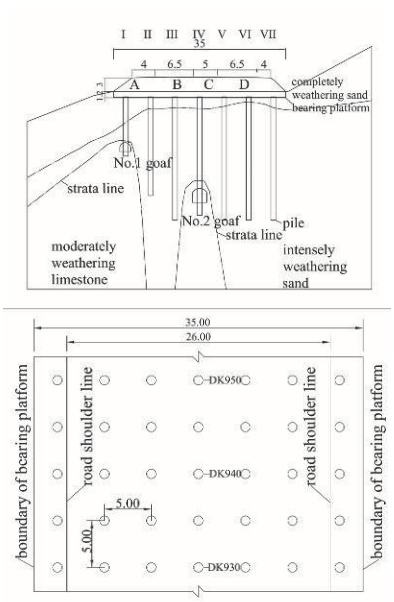


Fig.1 Location of strata, goafs and pile-plank arrangement (unit: m)

## 3. Model test

### 3.1 Model size and boundary conditions

Scale model was used to study the behavior of the pile-plank structure roadbed, and the geometrical resemblance constant $C_l$ was 25. The geometrical parameters are shown in Table 2.

Table 2 Geometry parameters of model

| Model elements | Prototype size/m | Model size/m |
|---|---|---|
| Width of roadbed | 26.0 | 1.040 |
| Thickness of bearing plank | 1.2 | 0.048 |
| Length of pile | 25 | 1.000 |
| Pile-to-pile distance | 5.0 | 0.200 |
| Height of No.1 goaf | 2.0 | 0.080 |
| Width of bearing plank | 35.0 | 1.400 |
| Height of fill materials | 3.0 | 0.120 |
| Diameter of pile | 1.0 | 0.040 |
| Width of goaf bottom | 2.5 | 0.100 |
| Height of No.2 goaf | 2.8 | 0.112 |

Compared with prototype, the model is affected remarkably by boundary conditions. As to the boundary conditions, Kishida made many tests in sand box to find an appropriate ratio of width to pile diameter (B/D) and that of distance between pile end and the bottom of

Table 3 Size of prototype and model

| Boundary | Prototype size/m | Model size/m | Remarks |
|---|---|---|---|
| Along railway | 25 | 1.0 | Considering the additional size which eliminate boundary effect |
| Across railway | 70 | 2.8 | Considering the additional size which eliminate boundary effect |
| Height | 45 | 1.8 | Height of padding +thickness of bearing plank +length of piles, and considering the additional size which eliminate boundary effect |

the sand box to pile diameter (Z/D), and he believed that when B/D was more than 10 and Z/D was more than 6, the effect of boundary conditions could be neglected (Zhang, et al., 1990). Xie et al. (2005) proposed that the effect area of boundary was 3 times as large as the size of bearing plank, and the effect depth was 15 times of pile diameter by summarizing on site data of buried depth of pile group foundation, the size of bearing plank, and the range of effect of earth pressure. During the process of model test of diaphragm walls, Wen et al. (2007) assumed the effect area of boundary was 3 times larger than the size of bearing plank, and the effect depth was the largest value in the settlement calculation considering boundary conditions.

The sizes of model box in this paper are as follows: the ratio of width of the box to pile diameter B/D was 10, the distance between the pile end and the bottom of the model box was 15D, the length along railway was that of 5 row piles plus effect area, and the width across railway was that of roadbed and effect area. After considering boundary conditions, the sizes of model are listed in Table 3.

### 3.2 Materials

The deformations of piles are almost elastic, so the elastic modulus is firstly considered in choosing their similar materials. After a comparison with many other materials, PPR (pentatrico peptide repeats) was finally selected as the substitution of piles with 32 mm outer diameter, 23 mm inner diameter, and 0.962GPa elastic modulus. The bearing plank was constructed by using cast-in-site concrete to connect with piles.

There are 3 types soil in site, i.e. completely weathering sandstone, intensely weathering sandstone, and moderately weathering limestone. Uniformly graded fine and coarse sands substituted for completely weathering sandstone and intensely weathering sandstone respectively. Fine sands were also the similar materials of roadbed.

The moderately weathering limestone layer which spreads under the piles ends is the bearing layer, so the compressive strength and elastic modulus are main influential factors to consider when choosing its similar material. In the model test, composite materials consist of 1.00kg medium-coarse sands, 0.10kg gypsum and 0.04kg cements were used to build the bearing layer.

### 3.3 Model construction

After the construction of model box, the strata where piles and goafs were placed were cast. Same materials that substituted the moderately weathering limestone were used to build the goafs roofs. Next, the prefabricated roofs were connected with the goafs. Finally, the entire goafs (Fig.2) were completed. The bearing plank was constructed by using cast-in-site concrete as the last step of the model construction.

Fig.2 Fabrication of goafs

### 3.4 Monitoring instrument

Monitoring points were installed to collect the data of (1) pile axial force; (2) earth pressure; and (3) settlements. The resistance value of electric resistance strain gauge is $\left(119.9 \pm 0.1\right)\Omega$ , and the sensitivity ratio $K = \left(2.08 \pm 1\right)\%$ . The measuring range of the micro earth pressure cells installed under piles and between piles is 50kPa, and 400kPa of those installed on the top of piles. Micrometer gauges were used to monitor settlements, and the measuring range is 5 mm and precision is 0.001 mm.

The layout of the monitoring points is as follows: (1) micro earth pressure cells were installed between 2 piles and between 4 piles under the bearing plank to collect the data of earth pressure, and the numbers were

$T_1$~$T_4$. (2) The $C_{j1}$ and $C_{j2}$ settlement monitoring points were set at the bottoms of No.1 and No.2 goafs roofs respectively. (3) There were another 4 settlement monitoring points ($C_{j3}$~$C_{j6}$) between 2 piles and between 4 piles under the bearing plank. (4) No.$C_{j7}$~$C_{j10}$ settlement monitoring points were set on the top of the bearing plank. (5) Resistance strain gauges were pasted along the No. Ⅰ~Ⅳ piles, and micro earth pressure cells were set on the bottom and the top of these piles, and the numbers were $T_5$~$T_8$. The layout is shown in Fig.3.

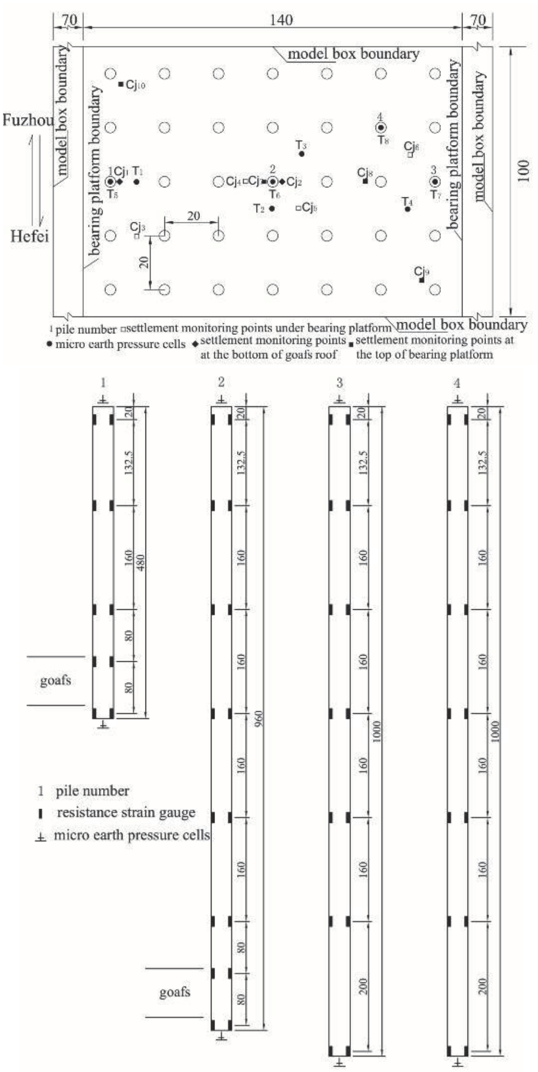


Fig.3 Monitoring points arrangement

### 3.5 Loads

The test loads included the gravities of fill materials above the bearing plank and ballastless track, train load and additional load. The dynamic load due to the running of the train can be determined by Formula (1).

$$P_d = \alpha P_j \tag{1}$$

Where: $P_d$ is dynamic load, and $\alpha$ is dynamic ratio, which equals 3.0 when the design speed is 300 km/h; and $P_j$ is static load.

In order to make detailed study of stress and deformations when the model subjected to loads, the loads were divided into 8 levels, i.e. 3 levels of fill materials loads, 3 levels of train loads, and 2 levels of additional loads. The details are shown in Table 4.

Table 4 Load on road embankment model

| Number | Load source | Load/kN | Loading mode |
|---|---|---|---|
| 1 | Fill materials | 1.12 | Gravity of fill materials |
| 2 | Fill materials | 2.24 | Gravity of fill materials |
| 3 | Fill materials | 3.36 | Gravity of fill materials |
| 4 | One train | 3.70 | Weights |
| 5 | Two trains | 4.03 | Weights |
| 6 | Four trains | 4.70 | Weights |
| 7 | Additional loads | 5.70 | Weights |
| 8 | Additional loads | 6.30 | Weights |

## 4、Results and analysis

### 4.1 Pile axial force

The pile axial forces of No.1~4 are shown in Fig.4. The axial force of No.1 pile declined as the depth increased, and remained constant when the pile passed through goafs. When the pile was subjected to the level 1 and level 2 loads, the axial force was small, even reached 0 at the base of the pile. By contrast, the axial force at the base was 0.061 kN, and at the top was 0.114 kN when the pile was subjected to the level 8 load. In that situation, the tip resistance accounted for 53.5% of the entire loads.

The trend of the No.2 pile axial force was similar to that of No.1 pile. The axial force at the base of the pile was 0.047 kN and that on the top was 0.119 kN when the level 8 load was imposed, and the tip resistance represented 39.5%, while the proportion of the skin friction was 60.5%, indicating that skin friction borne more loads as the length of piles increased.

No. 3 and No.4 piles do not pass through goafs. The axial forces decreased faster than those of No.1 and No.2 piles with the increase of piles depth, because the bearing layers supported No.1 and No.2 piles were mimic limestone, while that supported No.3 and No.4 were coarse sands which deformed relatively larger , as a result, skin friction was mobilized more.

### 4.2 Skin friction

Fig.5 shows the skin friction of No.1~4 piles. The skin friction of No.1 pile fell gradually along the pile, and reached 0 at the goafs. The entire skin friction accounted for 46.5% when the pile subjected to the

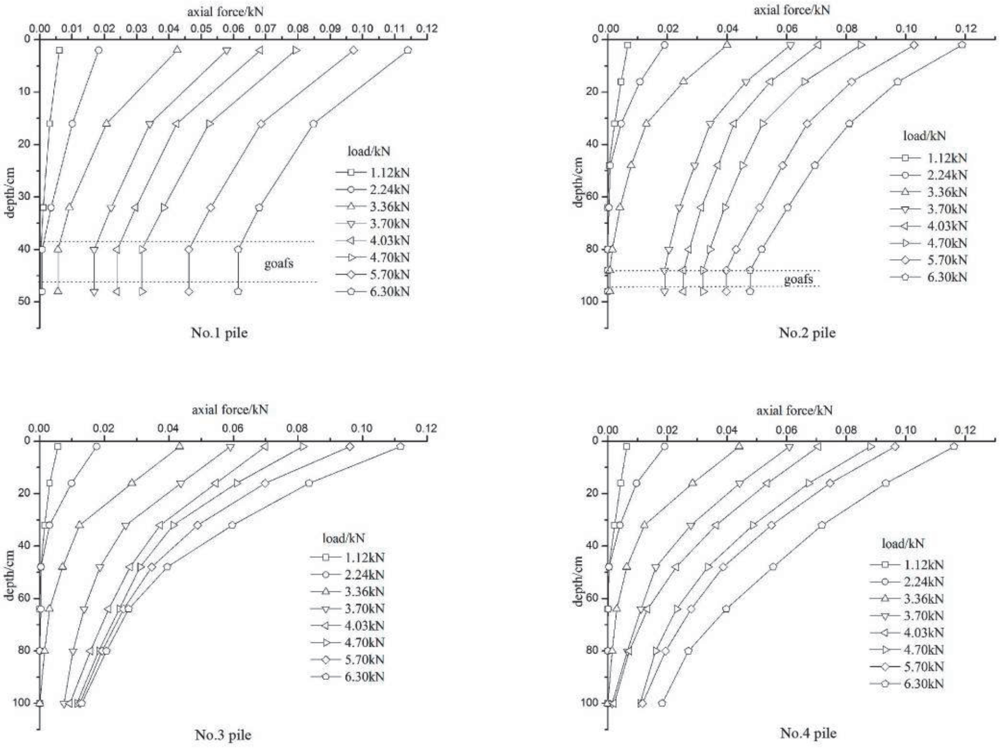


Fig.4 Distribution of axial force of piles

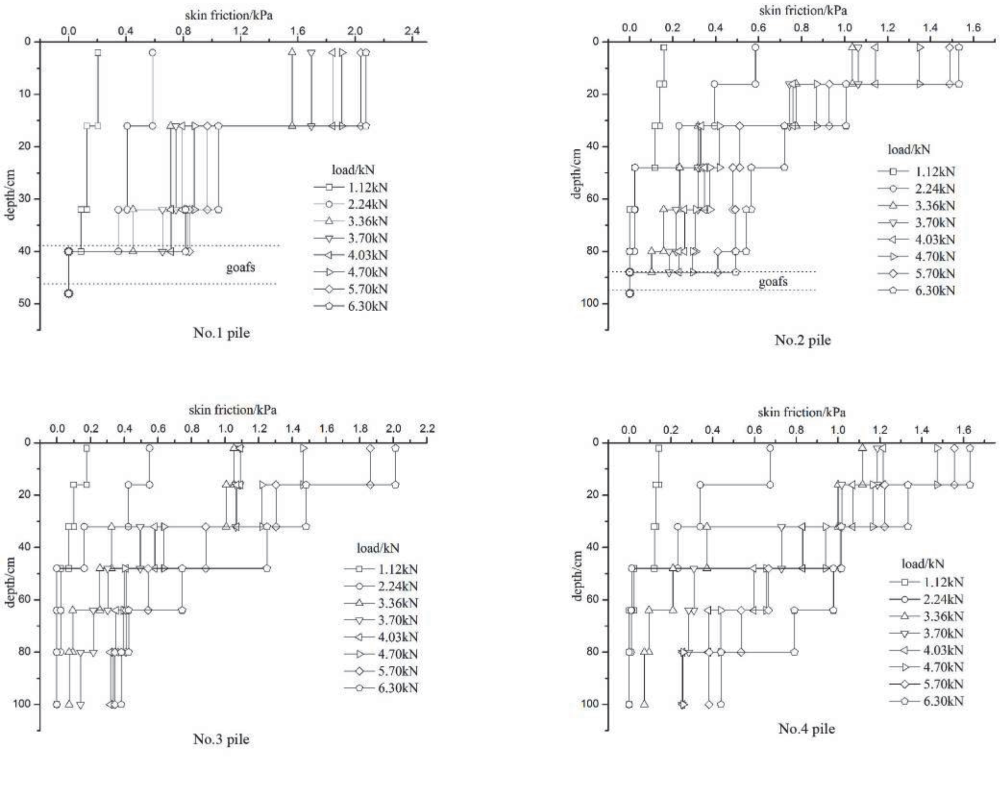


Fig.5 Skin friction of piles

level 8 load. The skin friction of No.2 pile made up 60.5% of the load, and the trend was similar to that of No.1 pile. Because of different pile lengths and different distributions of strata, the ratio of tip resistance to skin friction of No.1 piles distinguished from that of No.2 piles. When the load was small, there was no skin friction at the lower part of No.2 pile. With the increase of the loads, the skin friction was mobilized gradually. The skin frictions of No.3 and 4 piles also experienced a downtrend from the top to the base of piles. When the load was level 8, the proportion of skin friction of No.3 pile was 88.4%, bearing most of loads. The skin friction of No.4 pile experienced a similar trend due to same length and distribution of strata.

**4.3 Pile-soil stress**

The variation of earth pressure between piles is shown in Fig6. As depicted in the figure, there were 4 stages of earth pressure between piles with the growth of loads: when the loads were 0~3.36 kN, earth pressure went up steadily; when the loads were 3.36~4.03 kN, the rate of increase became lager; when the loads were 4.03~4.70 kN, the rate of increase dropped; when the loads were 4.70~6.30 kN, the rate of increase rose gradually to a constant value. These 4 stages suggested that there was a period of adjustment of earth pressure between piles, after that, the rate of increase remained stable at a constant value.

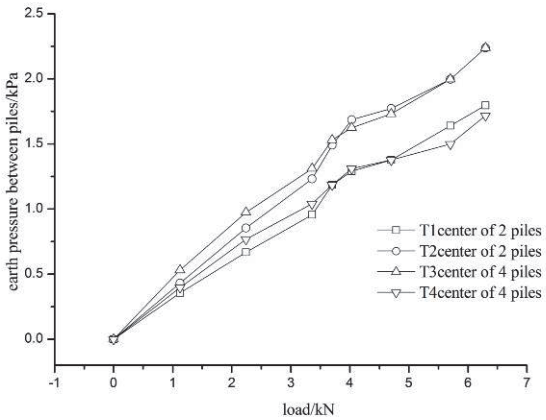


Fig.6 earth pressure between piles

Although the earth pressure between piles under different parts of bearing plank was similar, there were still slight distinctions. The trends of earth pressure between 2 piles and between 4 piles were same, however, the earth pressure between piles that were under the middle and the boundaries of bearing plank were different, and the middle one was larger than the boundaries.

The comparison of stress on the top and base of piles and earth pressure between piles is shown in Fig.7. At the initial stage of loading, the stress on the top of piles increased rapidly with increasing loads, after that, the stress went up gradually with a stable rate, suggesting that the loads borne by piles rose as the loads increased.

When the loads were small, the stress on the base of piles was 0, when the loads grew gradually, a part of loading transmitted to base, and the stress on the base increased, afterwards, such stress grew steadily. The stress on the bottoms of No.1 and 2 piles was larger than those of No.3 and 4 piles, because the skin friction of No.1 and 2 piles were smaller than those of No.3 and 4 piles when these 4 piles subjected to same loads.

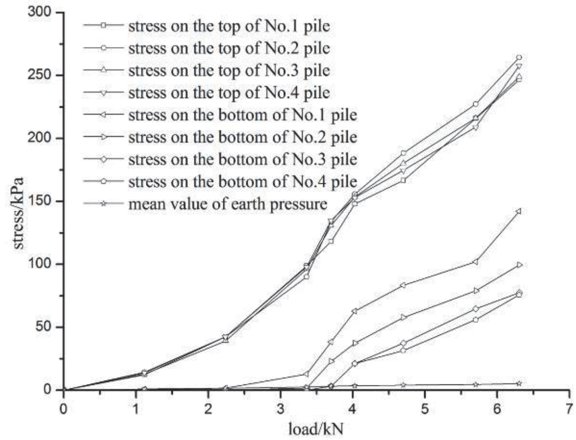


Fig.7 comparison of stress on top, bottom and earth pressure

The distinctions between stress on the top of piles and the earth pressure were pretty large, and the rate of increase of stress on the top of piles was larger, because the elastic modulus of piles was much larger than that of soils.

The pile-stress ratio is shown in Fig.8. The data was the mean value of stress on the top of piles and the mean value of earth pressure between piles. It is shown that the ratio increased from 31 when the load was 1.12 kN to 127 when the load was 30 kN, which indicated that piles borne more loads.

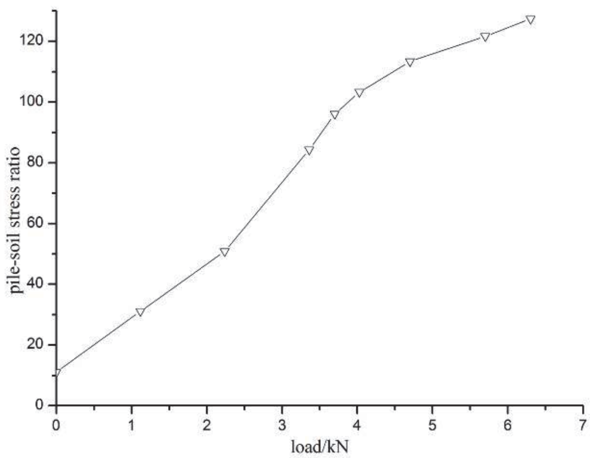


Fig.8 Pile-soil stress ratio

**4.4 Pile-soil load share ratio**

The pile-soil load share ratio is shown in Fig.9. The loads borne by piles increased with growth of loads. When the load was 1.12 kN, the pile load share ratio was 23.6%, because the deformation was small under that load, and the soil borne most loads. As the load increased, the deformation also increased, the stress of the piles increased remarkably due to large elastic modulus, as a result, the pile load share ratio increased to 50.6% when the load was 4.03 kN. The soil was mobilized gradually when the loads increased, which affected the pile-soil load share ratio. Finally, the pile load share ratio was 55.8%. We can also find that when the load was 4 kN, the two lines intersected because the loads supported by piles and soil both accounted for 50%.

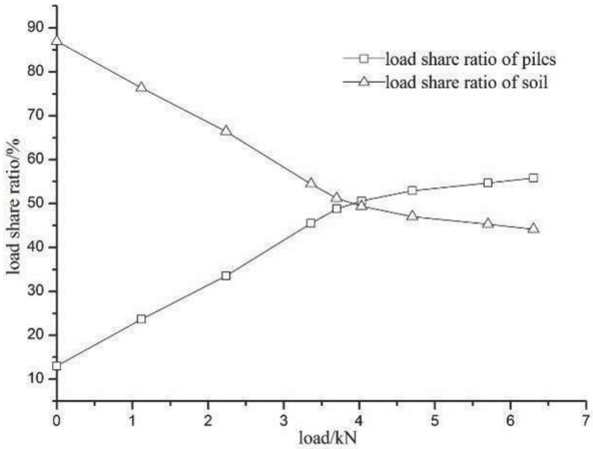

Fig.9 Pile-soil load share ratio

### 4.5 Settlements

The settlements of monitoring points are shown in Fig.10. The settlements of bearing plank and soils were both small, within an acceptable range. When the load increased from 1.12 kN to 6.30 kN, the settlements of bearing plank and soils increased from 0 to more than 0.13 mm. Although there was difference at different parts, the entire settlement was small, which meant that the bearing plank with a large stiffness control the different settlement well. What is more, there was no settlement at the roofs of No.1 and 2 goafs.

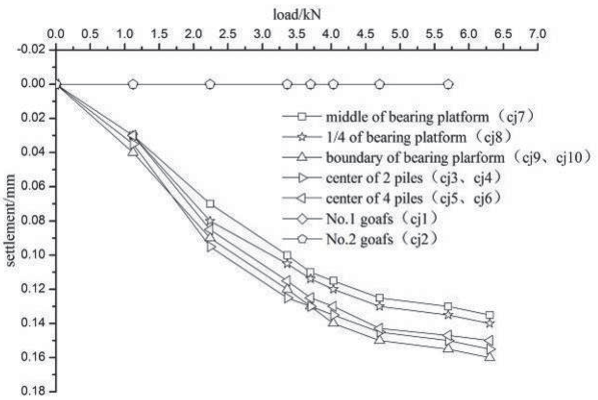

Fig. 10 Monitoring points settlements

### 4.6 Plank effect

Fig.4 also shows that the pile axial forces of 4 piles were similar when the piles subjected to same level load. For example, when the load was level 8 (6.30 kN), the axial forces were 0.11~0.12 kN. This phenomenon suggested that the bearing plank transmitted load uniformly to piles due to large stiffness. Besides, as depicted in Fig.10, the settlements of monitoring points on the bearing plank surface closed to each other except for the settlements of boundary points ($C_{j9}$ and $C_{j10}$), and all were smaller than the soil settlement, indicating that the bearing plank transferred the contact between roadbed and foundation from flexible to stiff and control the different settlement well.

## 5、 Conclusions

Based on the physical model test, this paper studies the behavior of pile-plank structures working as the composite foundation overlying goafs in a high speed railway. The main conclusions can be described as follows.

(1) The axial force on the top of piles was largest, and decreased rapidly at the upper part of piles. The axial force was constant when passing through goafs. The axial force on the tops of piles was similar when piles subjected to same load.

(2) The skin friction on the upper part of piles was larger, and was 0 at the goafs. There was no negative skin friction occurred.

(3) The change of pile-soil stress ratio was consistent with the pile-soil load share ratio. As the load increased, the rate of increase of loads borne by piles decreased gradually to a stable value.

(4) The settlements of bearing plank and soils increased rapidly at the initial stage, after that, the rate of increase decreased, and reached a stable value.

(5) With same load, the axial force of different piles closed to each other, because the bearing plank transmitted the load uniformly. Besides, the entire settlement of bearing plank was small, and the settlements at goafs and non-goafs were same.

(6) There was no deformation at the bottom of goafs roof, which meant that the bearing plank control the deformation well.

## References

Shen, Y., Li, X., Feng, R., et al. (2009): Settlement properties of pile-plank composite foundation in passenger dedicated line, Journal of Traffic and Transportation Engineering, Vol.9, No.6, pp. 32－35. [In Chinese with English abstract.]

Su, Q., Wang, W., Bai, H., et al., (2012): Bearing capacity mechanism of non-embedded pile-plank structure subgrade, Journal of Traffic and Transportation Engineering, Vol.12, No.1, pp. 19－24. [In Chinese with English abstract.]

Wen, H., Cheng, Q., Chen, X., et al., (2007): Study on bearing performance of rectangular closed diaphragm walls as bridge foundation under vertical loading, Chinese Journal of Geotechnical Engineering, Vol. 29, No.12, pp.1823-1830.[In Chinese with English abstract.]

Xie, T., Yuan, W., Ma, T., et al.,(2005): Model testing study on deformation behavior of super-large pile group under horizontal load, Chinese Journal of Rock Mechanics and Engineering, Vol.24, No.9, pp. 1582－1587. [In Chinese with English abstract.]

Xu, L., Wang, H., Zuo, S., et al., (2012): Test study of performance of composite pile foundation of high-speed railway controlling settlement, Rock and Soil Mechanics, Vol.33, No.9, pp. 2605 - 2612. [In Chinese with English abstract.]

Zhan, Y., Jiang, G., Niu, G., et al., (2007): Theoretical exploration on design of pile-plate structure in high steep slope on Wuchang-Guangzhou railway passenger dedicated line, Journal of Railway Engineering Society, Vol.24 (Supp.), pp. 94 - 101. [In Chinese with English abstract.]

Zhan, Y., Jiang, G., Niu, G., et al., (2008): Model experimental research on dynamic performance of pile-plank embankment, Rock and Soil Mechanics, Vol.29, No.8, pp. 2097 - 2010. [In Chinese with English abstract.]

Zhang, J., Zeng, J., Tu, Y., et al., (2011): Experimental study on CFG pile-raft composite foundation of Beijing-Shanghai high-speed railway, Journal of the China Railway Society, Vol.33, No.1, pp. 83 - 88. [In Chinese with English abstract.]

Zhang, S., Deng, A., Li, S. (1990): Study on model testing technique for socketed piles in soft rock, Journal of Chongqing Institute of Architecture and Engineering, Vol.12, No.3, pp. 68 - 75. [In Chinese with English abstract.]